AsiaRiceYield4km: Seasonal Rice Yield in Asia from 1995 to 2015

Huaqing Wu[1,2★], Jing Zhang[1,3★], Zhao Zhang[1,2], Jichong Han[1,2], Juan Cao[1,2], Liangliang Zhang[1,2], Yuchuan Luo[1,2], Qinghang Mei[1,2], Jialu Xu[2], Fulu Tao[4,5]

[1]Key Laboratory of Environmental Change and Natural Disasters, Ministry of Education Beijing Normal University, Beijing 100875, People's Republic of China

[2]School of National Safety and Emergency Management, Beijing Normal University, Beijing 100875 / Zhuhai 519087, People's Republic of China

[3]Faculty of Geographical Science, Beijing Normal University, Beijing 100875, China

[4]Key Laboratory of Land Surface Pattern and Simulation, Institute of Geographical Sciences and Natural Resources Research, Chinese Academy of Sciences, Beijing, 100101, People's Republic of China

[5]College of Resources and Environment, University of Chinese Academy of Sciences, Beijing 100049, People's Republic of China

★These authors contributed to the work equally and should be regarded as co-first authors.

Correspondence to: Zhao Zhang (zhangzhao@bnu.edu.cn)

Abstract. Rice is the most important staple food in Asia. However, high-spatiotemporal-resolution rice yield datasets are limited over this large region. The lack of such products greatly hinders studies that are aimed at accurately assessing the impacts of climate change and simulating agricultural production. Based on annual rice maps in Asia, we incorporated multi-sources predictors into three machine learning (ML) models to generate a high-spatial-resolution (4km) seasonal rice yield dataset (AsiaRiceYield4km) from 1995 to 2015. Predictors were divided into four categories that considered the most comprehensive rice growth conditions and the optimal ML models was determined based on an inverse proportional weight method. The results showed that AsiaRiceYield4km achieves good accuracy for seasonal rice yield estimation (single rice: R^2 = 0.88, *RMSE* = 920 kg/ha, double rice: R^2 = 0.91, *RMSE* = 554 kg/ha, and triple rice: R^2 = 0.93, *RMSE* = 588 kg/ha). Compared with single rice of Spatial Production Allocation Model (SPAM), the R^2 of AsiaRiceYield4km was improved by 0.20 and *RMSE* was reduced by 618 kg/ha on average. In particular, constant environmental conditions including longitude, latitude, elevation, and soil properties contributed the most (~45%) to rice yield estimation. For different rice growth periods, we found that the predictors of the reproductive period had greater impacts on rice yield prediction than those of the vegetative period and the whole growing period. AsiaRiceYield4km is a novel long-term gridded rice yield dataset that can fill the unavailability of high-spatial-resolution seasonal yield products across major rice production areas and promote more relevant studies on agricultural sustainability worldwide. AsiaRiceYield4km can be downloaded from an open-data repository (DOI: https://doi.org/10.5281/zenodo.6901968; Wu et al., 2022).

1 Introduction

As one major staple crop, rice (*Oryza sativa* L.) provides more than a quarter of calories for approximately half of the population with only 11% of the arable land on the earth (Maclean et al., 2002; Alexandratos and Bruinsma, 2012; Birla et al., 2017; Qian et al., 2020). Asia produces and consumes more than 90% of the global rice (Bandumula, 2018), which is dominated by poor smallholder farmers. Therefore, information on rice yield in Asia is essential for sustaining food security and farmers' livelihoods (Laborte et al., 2017). In the last half-century, the growth of rice yields has contributed more to an increase in production than the expansion of planting areas (Blomqvist et al., 2020) and will remain a dominant factor considering the land-use policies for reducing environmental pressure (Lambin and

Meyfroidt, 2011; Kim et al., 2021). In addition, Asia has complex rice cropping systems where rice may be cultivated multiple times within one year (Zhang et al., 2020a). It is critically necessary to identify the long-term and seasonal Asia rice yields – at high spatial resolution to monitor and guide agricultural production.

Previous global-scale crop yield datasets, including Harvester Area and Yields of 175 crops (M3Crops) (Monfreda et al., 2008), Spatial Production Allocation Model (SPAM) (You and Wood, 2006; Yu et al., 2020), Global Dataset of Historical Yields of Major Crops (GDHY) (Iizumi et al., 2014; Iizumi and Sakai, 2020), and Global Gridded Crop Model Intercomparison (GGCMI) phase 1 (Müller et al., 2019), have been produced and widely employed in many studies (Folberth et al., 2020; Kaltenegger and Winiwarter, 2020; Iizumi et al., 2021; Lin et al., 2021; Liu et al., 2021b). However, due to the different research goals and technical restrictions, their spatial resolutions are relatively coarser (e.g. ~10km for M3Crops and SPAM; ~55km for GDHY and GGCMI phase 1) and temporal resolutions are mostly annual (Laborte et al., 2017). Only a few datasets have seasonally temporal information (e.g., GDHY) but still cannot cover all rice seasons (Kim et al., 2021). In addition, the time spans are limited (e.g., only one year for M3Crops; every five years for SPAM). For the long-term rice yield dataset, GDHY, the authors used a fixed rice area basemap that did not obtain the interannual spatial dynamics of rice yield. To the best of our knowledge, a long-term seasonal rice yield dataset with higher spatial resolution and dynamic spatial distribution is currently unavailable for the major rice planting regions on the world.

To address the above issues, there is a significant need to acquire multi-sources data and wiser technologies for rice yield estimation (Chlingaryan et al., 2018; Cao et al., 2020; van Klompenburg et al., 2020; Zhang et al., 2020b; Chen et al., 2022). With the rapid development of remote sensing technology in recent years, large-scale and long-term high-spatiotemporal observations provide ample and timely phenological and growing information for rice growth. Ground-based data such as climate and soil also provide more key environmental information (Folberth et al., 2016; Zhang et al., 2021). Many publications that successfully combine satellite-derived data and ground environmental information for yield estimation have expanded our knowledge (Huang et al., 2013; Mosleh et al., 2015; Cao et al., 2021; Fernandez-Beltran et al., 2021). Nevertheless, few studies have yet employed annual paddy rice areas for yield estimation. Moreover, machine learning (ML), such as random forest (RF), extreme gradient boosting (XGBoost), and long short-term memory (LSTM) has been

increasingly and successfully used in crop yield estimation (Cai et al., 2019; van Klompenburg et al., 2020; Sakamoto, 2020; Luo et al., 2022). Such ML models can overcome the drawbacks of two traditional estimation methods: process-based crop models (PCMs) and statistical regression methods (SRMs). Compared with PCMs, ML can wisely select input variables according to the actual requirements and local geographical environment conditions without complicated parameters (Jeong et al., 2022). Due to the complex functions with higher efficiency and flexibility, the yield estimation results of ML are always better than those of SRMs (Chlingaryan et al., 2018). In addition, ML has a good spatial generalization. Therefore, ML models combined with multi-sources data potentially provide a good chance for large-scale gridded yield estimation and their accuracy improvement.

Overall, we would integrate multi-source data and annual rice maps into ML models for generating a seasonal rice yield dataset at 4km resolution across Asia (AsiaRiceYield4km) from 1995 to 2015. AsiaRiceYield4km will better support agricultural monitoring systems and related research over a large scale because of its higher-spatiotemporal resolution and longer-time span.

2 Materials and methods

2.1 Study area

Asia is the most important rice-producing area accounting for 89% of the planting area and 91% of the global production (Food and Agriculture Organization of the United Nations, FAO, 2022). Considering the accessibility of locally census-based rice yield data, 14 main rice-producing countries of Asia were selected and then divided into 27 cases (one case refers to one specific rice-cropping period in a country) based on different rice cropping systems (single, double, and triple rice), as shown in Fig. 1.

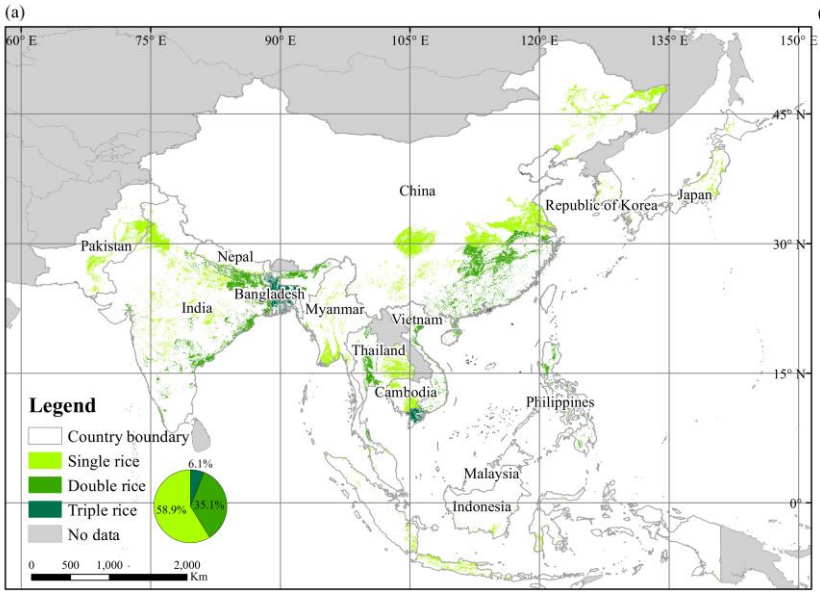

(b)

Country	Case number	Cropping systems (rice seasons)
Cambodia	1	Single (Single)
China	2	
India	3	
Indonesia	4	
Japan	5	
Malaysia	6	
Myanmar	7	
Nepal	8	
Pakistan	9	
Republic of Korea	10	
Thailand	11	
China	12	Double (Early, Late)
	13	
India	14	
	15	
Philippines	16	
	17	
Thailand	18	
	19	
Vietnam	20	
	21	
Bangladesh	22	Triple (Spring, Autumn, Winter)
	23	
	24	
Vietnam	25	
	26	
	27	

Figure 1: (a) Rice planting areas with different cropping systems in the main rice-producing countries of Asia. The green area represents the maximum paddy rice area where paddy rice grew for at least one year during the period 1995-2015 (Han et al., 2021, 2022). The pie chart represents the area proportion of different rice cropping systems. (b) Case numbers and cropping system for each country. Double rice follows the order of early before late (e.g., 12 and 13 represent the early season rice and late season rice in China, respectively), and triple rice follows the order of spring, autumn, and winter (e.g., 25, 26, and 27 represent the spring season rice, autumn season rice and winter season rice of Vietnam, respectively).

2.2 Data

Multi-sources data were collected for rice yield estimation, including annual rice area maps, rice yield of 1400 administrative units (minimum administrative division scale units for each country with available rice yield), leaf area index (LAI) information from remote sensing products, and rice growth environmental conditions (location, time, soil, and climate). In addition, considering the necessity of phenological information, we also produced gridded key phenological dates from LAI data based on inflection-based and threshold-based methods (Sect. 2.3.1). Except for yield records at administrative unit scale from official statistics (Table S1), the other data were resampled to 4km×4km by the nearest neighbour resampling method in ArcMap 10.2 (originally spatial information is listed in Table S2).

2.2.1 Rice area maps

We selected the latest public rice distribution map dataset, APRA500 (annual dataset of paddy rice area at a 500m resolution from 2000 to 2020), in this study (Han et al., 2021, 2022). APRA500 has annual rice distribution information which can reduce the influence of other land cover types. Due to the

topography conditions, cloud contamination, and the mixed-pixel effects with fragmented cropland fields, rice area in APRA500 was somehow underestimated (Han et al., 2022). To reduce this effect, we used the rice area union of the three years (current year, last year, and next year) to represent the rice area of the current year (e.g., the area of 2005 is the union of 2004, 2005, and 2006). Specifically, the union area of 2000, 2001, and 2002 was also applied to the years from 1995 to 2000 because of the unavailable area maps.

2.2.2 Seasonal rice yield

Rice seasons were determined mainly based on RiceAtlas (Laborte et al., 2017). RiceAtlas is the most comprehensive and detailed database for rice season and has been widely used in many studies (van Oort and Zwart, 2018; Muehe et al., 2019; Fritz et al., 2019). The United States Department of Agriculture (USDA, https://ipad.fas.usda.gov/ogamaps/cropcalendar.aspx, last accessed: 7 April 2022) and the national statistics of each country were also referenced for rice seasons determination. The rice seasons have various names in different countries, such as Aman, Aus, and Boro for triple rice of Bangladesh and Rabi and Kharif for double rice of India. To make the data more readable and consistent, we used single rice (single season), double rice (early and late seasons), and triple rice (spring, autumn, and winter seasons) for the three rice cropping systems in our study, as shown in Fig.1b. A few rice seasons (e.g., the early season in Cambodia, Malaysia, Myanmar, and Indonesia; and the winter season in India) were not considered due to the lack of yield records.

We collected seasonal rice yield data from FAO and other government websites (Table S1). Over 45000 rice yield records of 1400 administrative units from 1995 to 2015 were collected. The quality of these data has been checked and some yield outliers were filtered out according to the following rules: (a) exceeding the actual biophysically attainable yields and (b) beyond the averages ± two times variance during the period 1995-2015 (Zhang et al., 2014; Cao et al., 2020, 2021).

2.2.3 Key phenological dates

The transplanting, heading, and maturity dates are the three most important phenological dates during rice growing period. The whole growing period (WGP) is divided into two periods according to the three key phenological dates: vegetative period (VEP, from transplanting to heading) and reproductive period (REP, from heading to maturity). However, most rice phenology datasets are always

at administrative scales without interannual variation. The USDA provided country-scale growing phenological information. RiceAtlas had subnational phenology information but disregarded the annual dynamics (Laborte et al., 2017). In addition, these datasets lack heading date information about rice. Here, we retrieved the three dynamic key rice phenological dates from remote sensing data in Asia during the period 1995-2015 at a 4km×4km grid scale by inflection-based and threshold-based methods (Sect. 2.3.1). The USDA and RiceAtlas datasets provided a threshold range for phenology and were used to validate our extracted phenological dates.

2.2.4 Location and time

Location information includes longitude (*Lon*), latitude (*Lat*), and elevation (*Ele*). The Global 30-arc-second (1km) gridded Digital Elevation Model (DEM) dataset (1999) from the National Oceanic and Atmospheric Administration (NOAA) was employed in this study. The *Lon* and *Lat* information was collected from the centroid of each resampled 4km pixel by ArcMap 10.2. The temporal information is represented by the year (1995-2015).

2.2.5 Soil data

Soil properties are important factors controlling rice growth and final yield. The Harmonized World Soil Database (HWSD) v1.2 provides key soil property variables, including: Topsoil Sand Fraction (*T_Sand*), Topsoil Silt Fraction (*T_SILT*), Topsoil Clay Fraction (*T_CLAY*), Topsoil Reference Bulk Density, (*T_BULK_DEN*), Topsoil Organic Carbon (*T_OC*), and Topsoil pH (H2O) (*T_PH_H2O*) (https://www.fao.org/soils-portal/soil-survey/soil-maps-and-databases/harmonized-world-soil-database-v12/en/, last accessed: 7 April 2022; Wieder et al., 2014).

2.2.6 Climate data

TerraClimate (Abatzoglou et al., 2018), a monthly high spatial resolution (4km) meteorological dataset (http://doi.org/10.7923/G43J3B0R, last accessed: 7 April 2022) from 1995 to 2015, was used in our study. This dataset provides climate and water balance information for Asia rice (Salvacion, 2022), including Palmer Drought Severity Index (*PDSI*), precipitation accumulated (*Pre*), downward surface shortwave radiation (*Srad*), maximum temperature (*Tmax*), minimum temperature (*Tmin*), vapor pressure (*Vap*), and wind speed (*Ws*).

2.2.7 LAI

Remote sensing indices have been widely used in rice yield estimation (Son et al., 2020; Arumugam et al., 2021), but few studies have been conducted before 2000 (Liu et al., 2021a). To extend the period of the gridded yield dataset from 1995 in this study, we adopted Global Land Surface Satellite (GLASS) Advanced Very-High-Resolution Radiometer (AVHRR) LAI data (http://glass.umd.edu/Download.html, last accessed: 7 April 2022; Xiao et al., 2013, 2016, 2017), which begun from 1981 with a fine spatial resolution of 4 km and temporal resolution of 8 days. Compared with other similar products, GLASS AVHRR LAI has the highest accuracy and lowest uncertainty (Liang et al., 2021). The GLASS AVHRR LAI was used for rice phenological information extraction and yield estimation.

2.3 Methods

We applied three steps to generate AsiaRiceYield4km by incorporating multi-sources data into three ML methods: determining phenological dates, categorizing and selecting predictors, and developing the optimal models and generating gridded rice yield (Fig. 2). Details of each step are provided in the following sections.

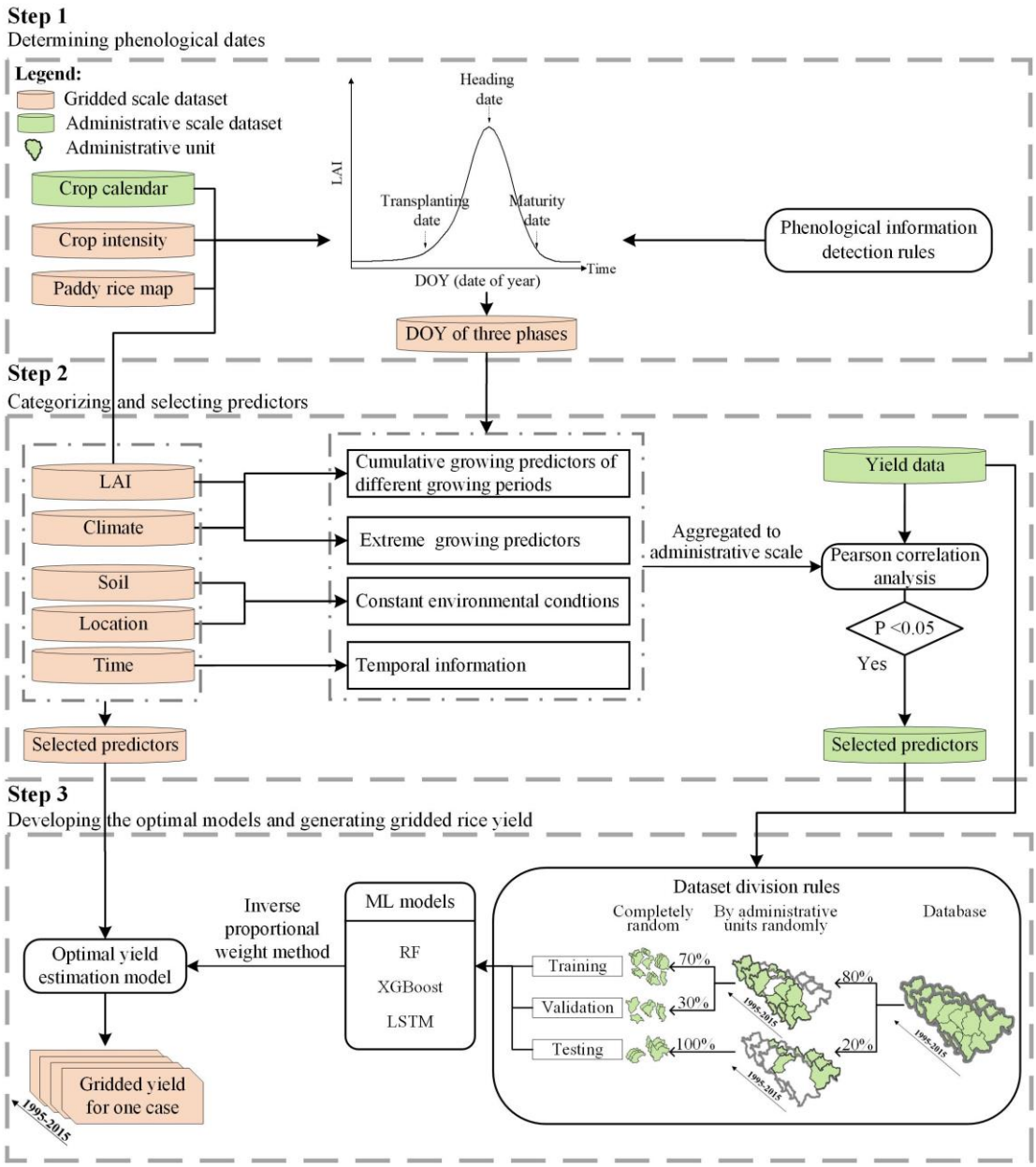

Figure 2: Flowchart for generating long-term and high-resolution gridded rice yields by incorporating multi-sources data into ML models for one case. All 27 cases followed these steps and were combined to get the AsiaRiceYield4km dataset.

2.3.1 Determining phenological dates

The inflection-based method (Chen et al., 2016; Luo et al., 2020a) and threshold-based method (Manfron et al., 2017) were employed to detect rice phenological dates (Fig.2 step1) according to the following rules: (1) Transplanting dates: The LAI always maintains a low value for a period before the transplanting date and dramatically increases after this date (Sakamoto et al., 2005; Chen et al., 2018). Therefore, if there is one point in the LAI curve where the first derivative is > 0 after it or its second derivative is equal

to 0, this point is defined as the transplanting date. (2) Heading dates: the inflection point from VEP to REP (Wang et al., 2018) is characterized by the maximum value of the LAI between the transplanting date and the maturity date (Son et al., 2013). (3) Maturity dates: the physiological activity of rice will sharply drop during the harvesting period. The first inflection point at the LAI curve where its first derivative becomes negative is considered the maturity date. In addition, LAI values of pixels beyond the averages ± two times standard deviation (SD) were filtered (Zhang et al., 2022). If the phenological dates in some grids cannot be detected by the above rules or be filtered, the average value of the administrative unit where the grids are located is applied.

2.3.2 Categorizing and selecting predictors

To provide comprehensive rice growth information for the ML models, we divided the multi-sources data into four categories including 50 predictors (Table S3): cumulative growing predictors of different growing periods (CGP), extreme growing predictors (EGP), constant environmental conditions (CEC), and temporal information (TI) (Fig. 2 step2). The CGP includes the sum of each LAI and climate variable in different growing periods (VEP, REP, and WGP), reflecting the overall growing and weather difference of the three continuous growing periods. The EGP consists of the maximum and minimum of each climate and LAI variable considering the impact of extreme events. CEC reflects the influence of the geographical environment on rice growth. TI reflects long-term agronomic technology improvements and variety renewal (Huntington et al., 2020). All these predictors were aggregated to administrative scale. The predictor values of grids located in one administrative unit were averaged to this administrative unit.

High-dimensional predictors often affect the accuracy and computational efficiency of ML methods (LeCun et al., 2015; Zhang et al., 2019). To reduce this effect, Pearson correlation analysis was employed to estimate the relationship between yield and other variables for each case. The variables with a significant correlation ($p < 0.05$) were selected as predictors (Cao et al., 2021). The yield and selected predictors of one case were input into one model. Specifically, the four predictors, *Lon*, *Lat*, *Ele*, and *Year*, were considered to have a stable impact on rice yield and were included in all 27 estimation models for the 27 cases (Ray et al., 2019; Huntington et al., 2020). Considering the covariate-relation of the

predictors in CGP for WGP and the remaining two periods, the predictors of WGP would be selected if its Pearson *R* was higher than that in the remaining two periods, or vice versa.

2.3.3 Developing the optimal models and generating gridded rice yield

(1) Dataset division rules

To effectively reduce overfitting effects (Dinh and Aires, 2022), we divided all data into three sets (training, validation, and testing) which were used to optimize the ML parameters, select the optimal model, and evaluate its generalization ability, respectively (Ripley, 2007). The diagram of the database division process is shown in Fig. 2 step3. For each case, the whole database contained the selected predictors from all administrative-scale units during 1995-2010. The database was randomly divided into two subsets by the administrative unit: 20% of the samples were used for testing and the remaining 80% were randomly resplit into 70% for training and 30% for validation without consideration of administrative units. Thus, the training, validation, and testing sets contain 56% (80%×70%), 24% (80% ×30%), and 20% (20%×100%), respectively, of the whole dataset. Such division rules avoid information leakage from the testing set to the training set (Meroni et al., 2021) and enhance the robustness of the model.

(2) ML models

ML can develop transfer functions based on the relationships between predictors and target variables for rice yield estimation (Chlingaryan et al., 2018; Shahhosseini et al., 2020). Three widely employed ML models, RF, XGBoost, and LSTM were selected for rice yield estimation. The RF is based on the bagging ensemble model, which generates multiple decision trees and obtains predictions by voting on all individual trees (Breiman, 1996, 2001). In addition, extra randomness is introduced to the RF when generating trees and searching for the best tree stages (Shahhosseini et al., 2020). It provides more diversity for trees and can generate the overall better performance model (Zhang et al., 2019). XGBoost uses the optimized gradient boost for decision trees, which tries to make weak learners strong (Chen and Guestrin, 2016). This method adopts an updated strategy to train the estimated model and the updated model minimizes the loss by reducing errors from previous models (Obsie et al., 2020). LSTM is a special recurrent neural network (RNN) that is proposed to overcome the vanishing and exploding gradient problems of RNNs (Hochreiter and Schmidhuber, 1997; Sak et al., 2014; Tian et al., 2021). LSTM

contains input, hidden and output layers and the hidden layers consist of memory cells (He et al., 2019; Zhang et al., 2019). Tuning hyper-parameters can effectively improve the accuracy for rice yield estimation (Shahhosseini et al., 2021). The hyper-parameters tuning details and Python library information of the ML algorithm are shown in Supplementary Methods.

(3) Model evaluation

The coefficient of determination (R^2) and root-mean-square error (*RMSE*) were adopted to evaluate the performance of each model for each case.

$$R^2 = 1 - \sum_{i=1}^{n}\left(Y_{i,j}^{ob} - Y_{i,j}^{es}\right)^2 / \sum_{i=1}^{n}\left(Y_{i,j}^{ob} - \bar{Y}_{i,j}^{ob}\right)^2 \quad (1)$$

$$RMSE = \sqrt{\sum_{i=1}^{n}\left(Y_{i,j}^{es} - Y_{i,j}^{ob}\right)^2 / n} \quad (2)$$

where i is the number of administrative units, n is the total number of administrative units, and j is the year. $Y^{ob}_{i,j}$ is the observed rice yield from government or FAO websites in the ith administrative unit of year j, $\bar{Y}^{ob}_{i,j}$ is the average of the observed rice yield in the ith administrative unit of year j, and $Y^{es}_{i,j}$ is the AsiaRiceYield4km yield in the ith administrative unit of year j.

(4) The optimal yield estimation model selection

In this study, three ML models can generate three different yield estimation results. Previous studies recommend the weighted ensemble method by combining the estimation results of different methods, wishing for a relatively stable result but still giving up some accuracy (Shahhosseini et al., 2020, 2021). Moreover, many studies also selected the optimal ML model by comparing only the accuracy of validation/testing sets (Zhang et al., 2021; Chen et al., 2022; Luo et al., 2022). Here, to conduct a comprehensive evaluation of different ML models and datasets, we developed an inverse proportional weight (IPW) method to assign weights for training, validation, and testing accuracy to calculate the adjusted accuracy for each ML model (Eq. 3-7). The ML model with the best adjusted accuracy was selected as the optimal ML model.

$$w_{tr} = p_{tr} / (p_{tr} + p_{va} + p_{te}) \quad (3)$$

$$w_{va} = p_{va} / (p_{tr} + p_{va} + p_{te}) \quad (4)$$

$$w_{te} = p_{tr} / (p_{tr} + p_{va} + p_{te}) \quad (5)$$

$$R^2_{ad} = R^2_{tr} \cdot w_{tr} + R^2_{va} \cdot w_{va} + R^2_{te} \cdot w_{te} \quad (6)$$

$$RMSE_{ad} = RMSE_{tr} \cdot w_{tr} + RMSE_{va} \cdot w_{va} + RMSE_{te} \cdot w_{te} \quad (7)$$

where *tr*, *va*, and *te* are abbreviations for training, validation, and testing; p_{tr}, $p_{va,}$ and p_{te} are the inverse proportions for the sizes of the training, validation, and testing sets, respectively, which are equal to 1/0.56, 1/0.24, and 1/0.20, respectively; and w_{tr}, w_{va}, and w_{te} are the weights of the training, validation, and testing sets, respectively. R^2_{ad} and $RMSE_{ad}$ represent the adjusted R^2 and *RMSE*, respectively. R^2_{tr}, $R^2_{va,}$ and R^2_{te} are the R^2 values of the training, validation, and testing sets, respectively; $RMSE_{tr}$, $RMSE_{va}$, and $RMSE_{te}$ are the *RMSE* values of the training, validation, and testing sets, respectively. The ML model with the highest R^2_{ad} and lowest $RMSE_{ad}$ is regarded as the optimal model for each season in Fig. 1b.

(5) Gridded rice yield generation

For each case, predictors of gridded scale consistent with administrative scale (Sect. 2.3.2) were input into the optimal model and the gridded rice yield was generated from 1995 to 2015. All the27 cases followed this process and were combined to generated the AsiaRiceYield4km dataset.

(6) Uncertainty spatialization

To provide the spatial uncertainty, the relative *RMSE* (*RRMSE*, Eq. 8) of AsiaRiceYield4km was calculated according to (Luo et al., 2020b). *RRMSE* of each administrative unit was allocated to the centroid of the unit and kriging interpolation method was used to spatialize the distribution of uncertainty.

$$RRMSE = \sqrt{\sum_{i=1}^{m}\left(\left(Y_{i,j}^{es} - Y_{i,j}^{ob}\right)/Y_{i,j}^{ob}\right)^2 / m} \cdot 100\% \quad (8)$$

where *m* is the total number of the year.

3 Results

3.1 Performance of the estimated models

After selecting the optimal ML model for each case, we scattered the seasonal training, validation, testing, and adjusted accuracy in Fig. 3. The training R^2 is higher than 0.9 for all cases, followed by validation and testing R^2 (average: 0.78 and 0.69, respectively). The R^2_{ad} ranges from 0.60 to 0.90 (average: 0.77), with the lowest R^2_{ad} in the single season of Malaysia and the highest R^2_{ad} in the winter season of Bangladesh (Fig. 3c). As for *RMSE*, the averages for training, validation, and testing are 105, 408, and 489 kg/ha, respectively. The $RMSE_{ad}$ ranges from 162 to 817 kg/ha and its average is 396 kg/ha. The highest $RMSE_{ad}$ is for single rice in China (Fig. 3d). The rice yields of China are mostly higher than those

of other countries, which might cause more modeling uncertainties. For double rice systems (Fig. 3b and 3e), there is no significant difference between their modeling accuracies, with approximately 0.77 for R_{ad}^2 and 410 kg/ha for $RMSE_{ad}$. For triple rice, the winter season in Bangladesh has the highest R_{ad}^2 (0.90; No. 24 dot in Fig. 3c), and the spring season in Vietnam has the lowest $RMSE_{ad}$ (327 kg/ha; No. 25 dot in Fig. 3c). Additionally, 27 optimal models consist of two types of ML models—XGBoost for 15 seasons and RF for 12 seasons—with no LSTM model. The 27 optimal models and their hyper-parameters are listed in Table S5.

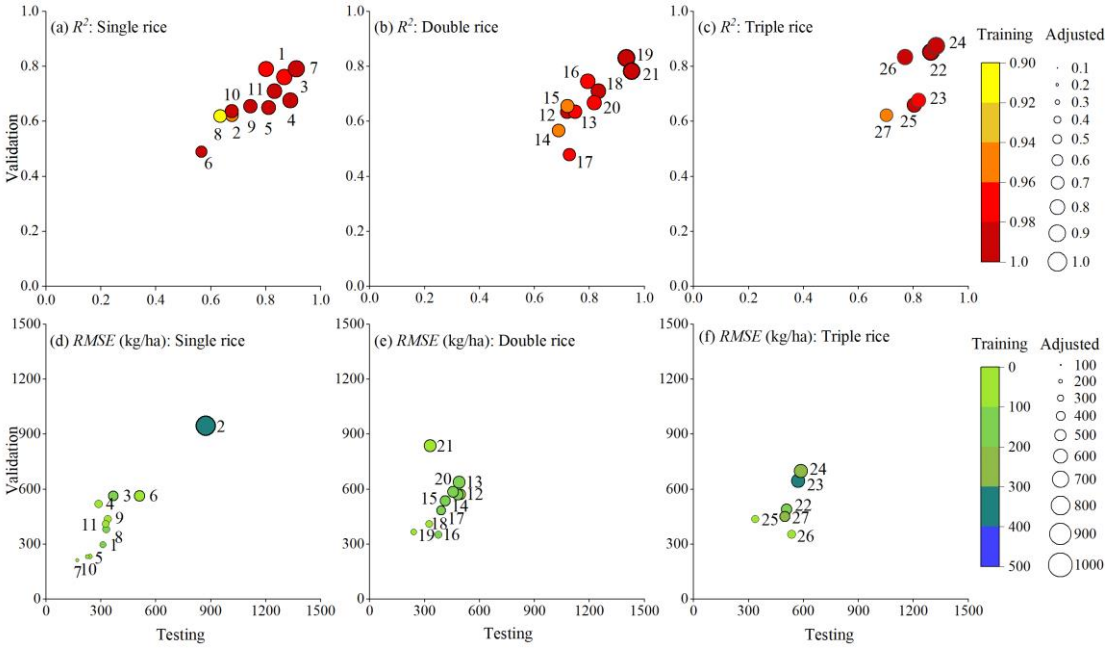

Figure 3: Accuracy (R^2 a-c and *RMSE* d-f) of the estimated yields for seasonal rice in each region. The R^2 (a-c) and *RMSE* (d-f) are presented in the top panel and bottom panel, respectively. The color of the dots indicates different training accuracy ranks; testing accuracy on the x-axis; validation accuracy on the y-axis; and the size of dots represents the adjusted accuracy. Note: numbers for each dot represent each case shown in Fig. 1b.

3.2 Comparing AsiaRiceYield4km products with the observations

After aggregating AsiaRiceYield4km into administrative units, we compared them with the observed yield at administrative and annual scales. At the administrative scale, comparisons were separately conducted for single, double, and triple rice, as shown in Fig. 4. The estimated and observed yields are closed around the 1:1 line. The overall R^2 is higher than 0.87, while the *RMSE* is lower than 921 kg/ha, suggesting that AsiaRiceYield4km is mostly identical to the observations. The accuracy of single rice (R^2: 0.88 and *RMSE*: 920 kg/ha) is slightly lower than that of double rice (R^2: 0.91 and *RMSE*: 554 kg/ha)

and triple rice (R^2: 0.93 and *RMSE*: 494 kg/ha), mainly because some high-yielding units are not well estimated for single rice (Fig. 4a). Moreover, late rice shows higher accuracy than early rice (R^2: 0.92 > 0.89, *RMSE*: 553 kg/ha < 556 kg/ha), which is consistent with the previous study (Cao et al., 2021). As for triple rice, winter rice has higher accuracy than spring and autumn rice even though its yield range was the greatest.

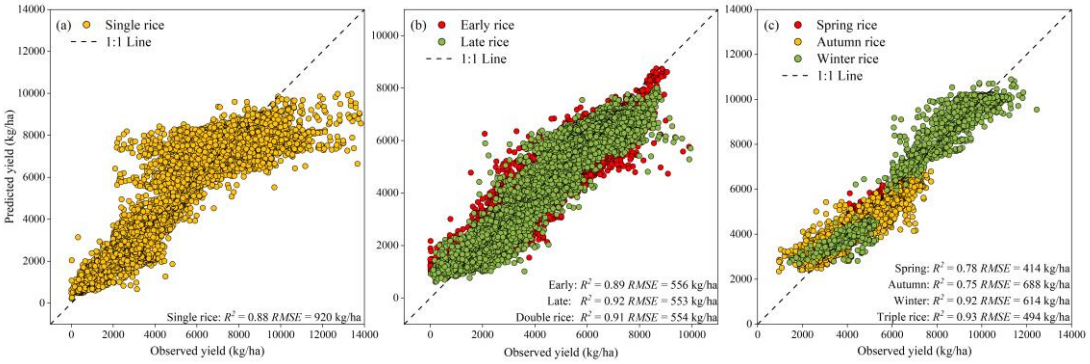

Figure 4: Comparison of AsiaRiceYield4km with observed yields at administrative units for (a) single rice, (b) double rice, and (c) triple rice.

At the interannual scale, annual average yield of AsiaRiceYield4km and observed yields for each case are presented. All seasons are statistically highly significant (p < 0.001), and R^2 of all the results is higher than 0.8. In addition, the differences of SD are also presented in Fig. 5. The largest difference is the early season for double rice in Vietnam which is mainly attributed to the underestimation of AsiaRiceYield4km after 2006. All differences of std are lower than 200 kg/ha, indicating that AsiaRiceYield4km can well estimate and capture the interannual variations in observed yields.

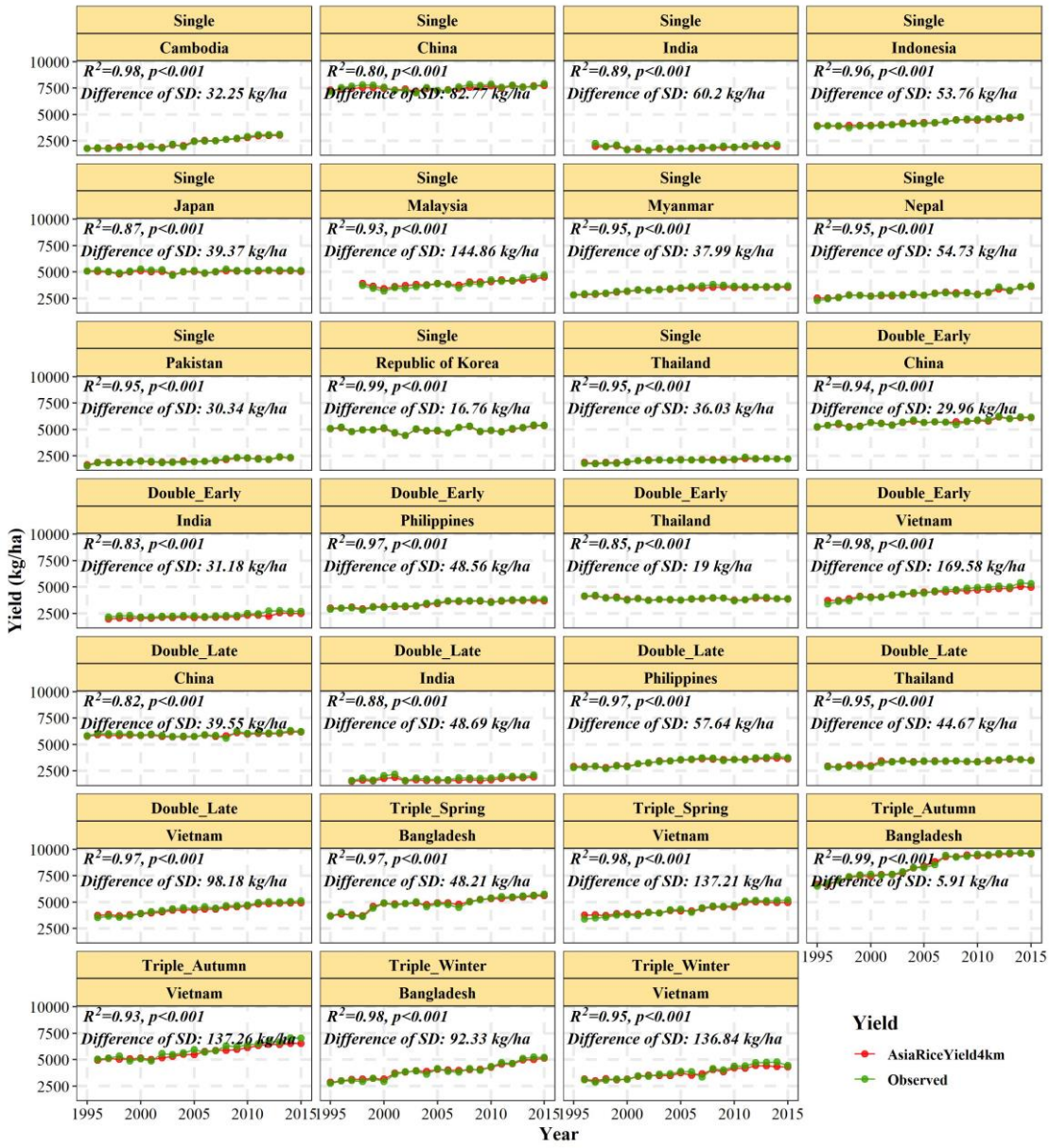

Figure 5: Interannual comparison of AsiaRiceYield4km with observed yield from 1995 to 2015.

3.3 Comparing AsiaRiceYield4km products with SPAM

Due to the limited time coverage and rice season information of SPAM, only single rice in 2000, 2005, and 2010 were compared between AsiaRiceYield4km and SPAM. The spatial distribution of rice yield for AsiaRiceYield4km, SPAM, and observed yield in 2005 are presented in Fig. 6a-c with the zoom-in views of the Indo - Gangetic Plain (IGP) in Pakistan and India (Fig. 6 a1-c1). After aggregating AsiaRiceYield4km and SPAM to administrative units, both products were also quantitatively compared with the observed yield in Fig. 6d for 2005. Similar comparisons for 2000 and 2010 are shown in Fig. S1. Compared with SPAM, AsiaRiceYield4km has a higher R^2 and a lower *RMSE*. Specifically, the R^2

of AsiaRiceYield4km is 0.18, 0.23, and 0.20 higher and the corresponding *RMSE* value is 570, 692, and 592 kg/ha lower, respectively, than that of SPAM in 2000, 2005, and 2010. Moreover, AsiaRiceYield4km shows better spatial consistency with the observed yield across the whole area. The yield spatial variation in AsiaRiceYield4km and the observed yield are identical in the IGP, while some administrative unit yields of SPAM are overestimated (Fig. 6a1-c1).

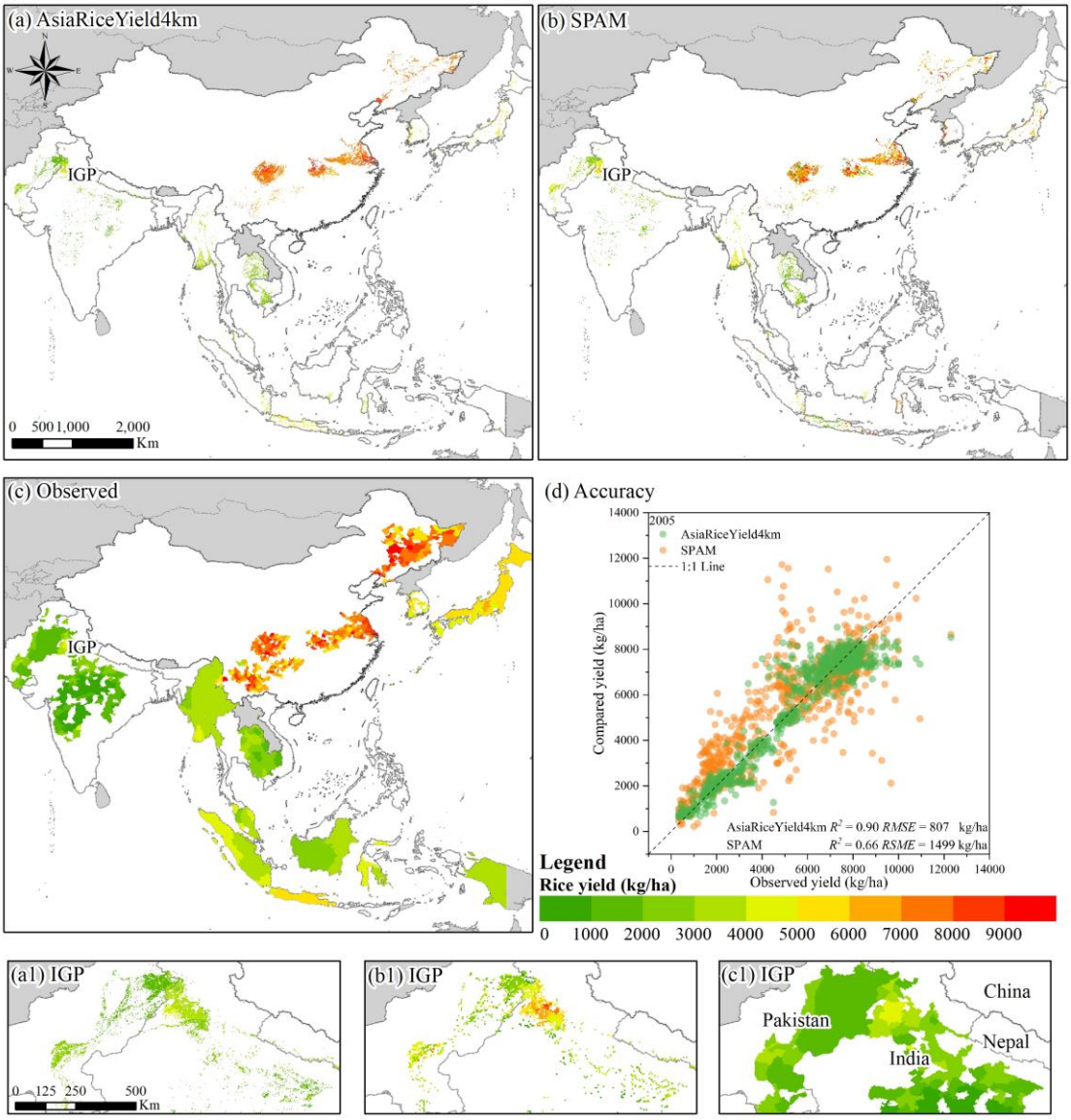

Figure 6: Yield distribution of (a) AsiaRiceYield4km, (b) SPAM, and (c) observed yields in 2005, and (d) quantitative comparisons with the observed yields in 2005. (a1) to (c1) are the zoom-in views of the IGP in Pakistan and India, with (a1) for AsiaRiceYield4km, (b1) for SPAM, and (c1) for the observed yields.

3.4 Spatiotemporal characterizations of AsiaRiceYield4km

Based on the estimated seasonal yields from optimal ML models, we characterized the spatiotemporal patterns of rice yields during the period 1995-2015. At the spatial scale, single rice is widely distributed

in 11 countries across the whole area, where its yield varies greatly from 400 to 10000 kg/ha with an average of 5428 kg/ha. Specifically, the highest average yield is in China (7384 kg/ha) and the lowest yield is in India (1889 kg/ha). Such a large difference might be ascribed to better irrigation in China (Dawe et al., 2010) and relatively low-level soil fertility, investment, and technology in India (Srivastava and Mahapatra, 2012). Double rice mostly distributed between 30°N~0°. Double rice has insignificant differences between early yield and late yield: early rice ranges from 1041 to 8347 kg/ha with an average yield of 4598 kg/ha; late rice ranges from 666 to 7977 kg/ha with an average yield of 4539 kg/ha. Triple rice seasons are planted in Bangladesh and Vietnam. The ranges of rice yield for spring, autumn, and winter are from 3034 to 6249, from 2690 to 6986, and from 2514 to 10870 kg/ha, with corresponding averages of 4153, 4716, and 7794 kg/ha, respectively. Notably, the highest average yield is 8597 kg/ha for winter rice in Bangladesh, due to its high-yielding hybrid varieties and well-managed fieldwork (e.g., fully irrigated increasing fertilizer, pesticides, and herbicides applications) (Meroni et al., 2021).

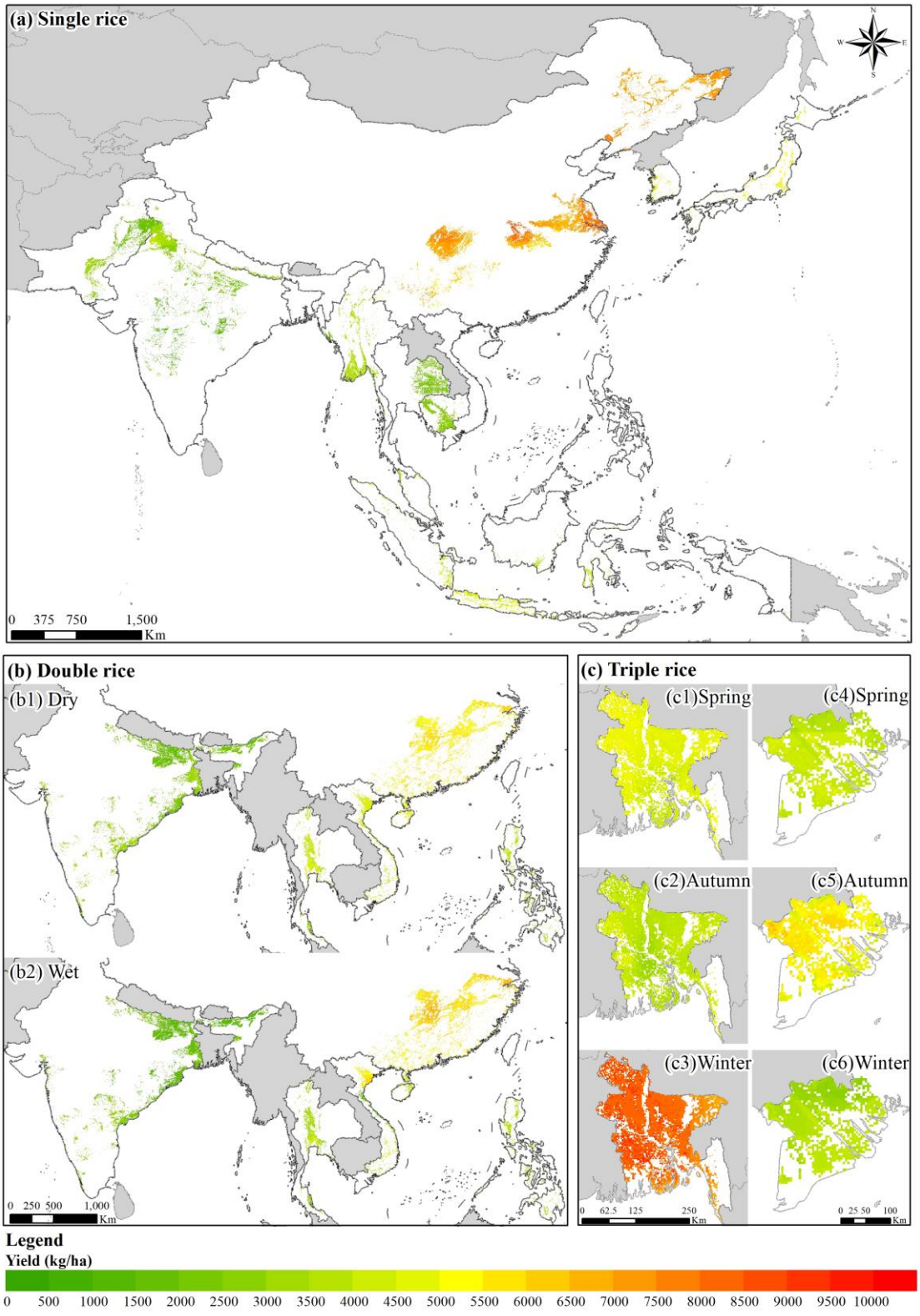

380

Figure 7: Spatial patterns of the estimated rice yields (averages during the period 1995-2015) for different seasons.

For the temporal scale, the interannual rate of yield change (defined as yield difference of last year and current year divided by yield of last year) from 1995 to 2015 for each case is shown in Fig. 8. The annual rate ranges from -18.55% to 25.57%. The average interannual rate during 1995-2015 increases for most cases, with the exception of single rice for Japan (-0.01%) and the early season of double rice for Thailand (-0.11%). Among all cases, the greatest average rate is 2.65% in Cambodia.

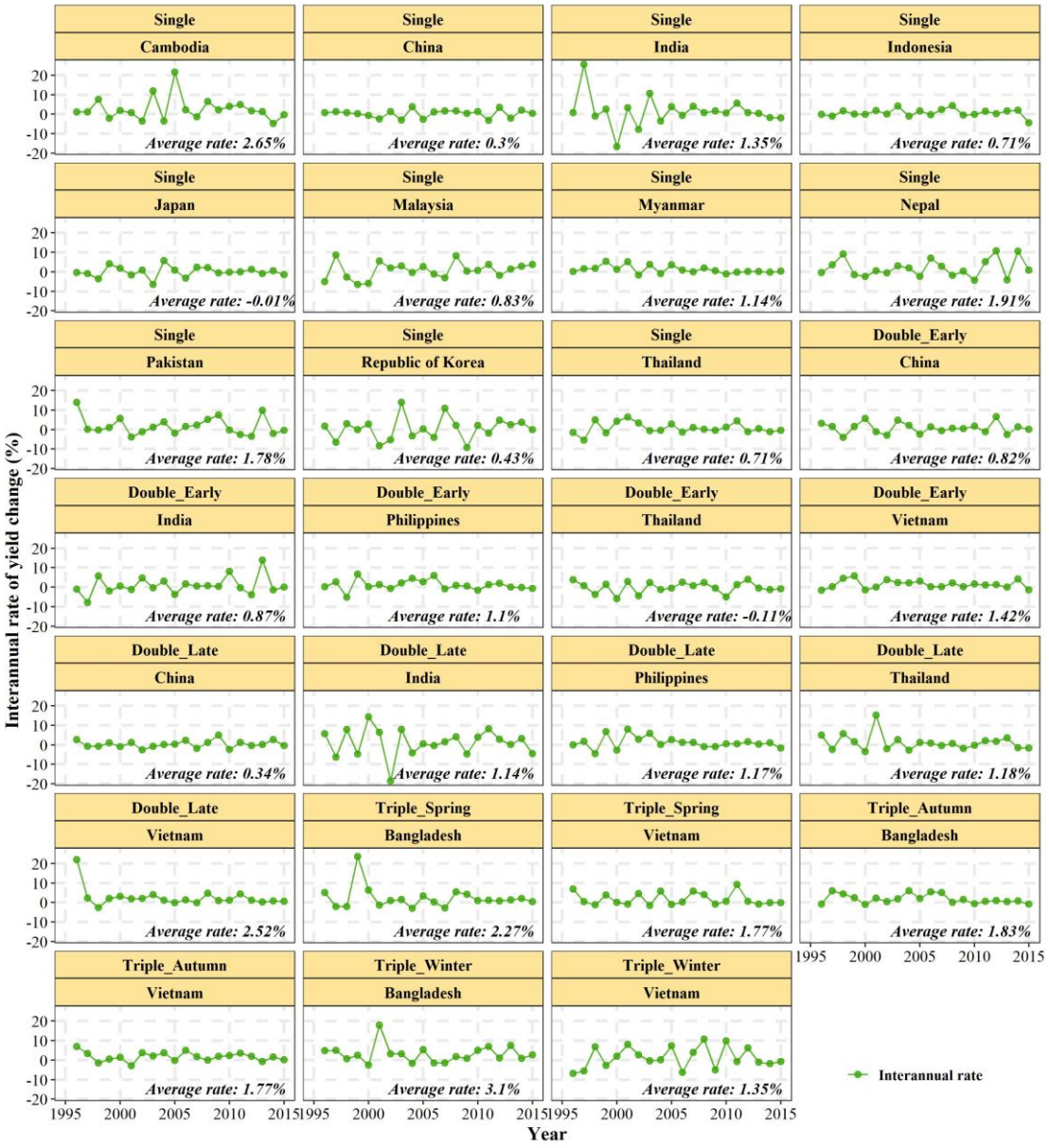

Figure 8: Temporal variation in the estimated rice yield change for different seasons from 1995 to 2015.

4 Discussion

4.1 Frequency and importance of the predictors in ML models

In this study, 50 predictors were used in ML models but their contributions greatly varied. First, only predictors having a significant correlation with yields were selected for ML models, with the exception of temporal and spatial predictors (*Year*, *Lon*, *Lat*, and *Ele*) (details in Sect. 2.3.2). As a result, the selection frequency of temporal and spatial predictors was 27 times and the selection frequency of other predictors ranged from 2 to 25 times (Fig. 9a). Using the selected predictors, ML models then estimated rice yields and ranked the importance of each predictor (Fig. 9a). The results showed that temporal and spatial predictors had relatively greater average importance (>0.05) and that the importance of the remaining predictors was lower than 0.03 (Fig. 9a).

For different growing periods, REP predictors had greater average importance (0.010) in ML models followed by WGP and VEP predictors (0.007 and 0.005). The average selection frequency for WGP and VEP predictors (8.4 and 10.9 times, respectively) was much lower than that of REP (14.5 times). Therefore, REP predictors contributed the most to yield estimation, which was also consistent with previous studies (Chang et al., 2005; Nazir et al., 2021). In addition, we also found that EGP predictors (0.014 and 21.3 times) had greater average importance and selection frequency than CGP predictors (0.007 and 11.3 times), respectively, indicating the stronger response of rice yields to extreme growth conditions.

Figure 9b further proportioned the importance of the four predictor categories for each seasonal rice. Although the proportioned importance varied for different rice seasons, the overall contribution was highest for CEC predictors (45%) followed by EGP (21%), TI (18%), and CGP predictors (16%). CEC had the greatest proportioned importance for most countries which suggested the great importance of the geographical environment for rice yield estimation. More interestingly, the importance of CEC predictors for Myanmar, Thailand, and the late season of Vietnam exceeded 0.8.

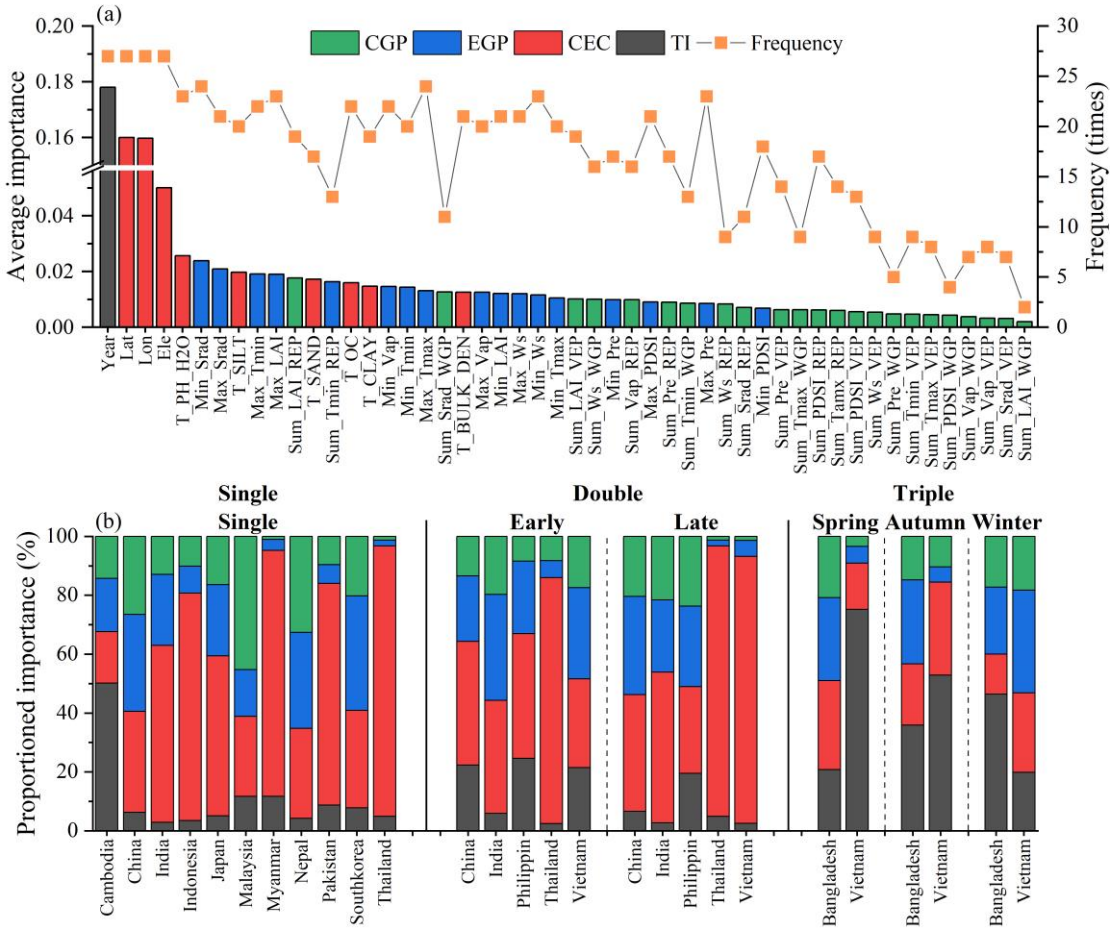

Figure 9: (a) Average frequency and importance of each predictor. (b) The proportioned importance of each predictor category for seasonal rice.

4.2 Improvements in AsiaRiceYield4km

AsiaRiceYield4km is a seasonal rice yield product with high spatiotemporal resolution and a long time span across the dynamic rice planting areas in the main rice-producing countries of Asia. Compared with SPAM, the spatial resolution of our AsiaRiceYield4km is 4km which is the current highest resolution among all rice yield datasets. Additionally, the product period covers from 1995 to 2015 and includes multi-seasonal rice yields within one year, with more information than most other rice yield datasets. Similarly, AsiaRiceYield4km considered both the annual dynamic change in rice-planting areas and phenological information at a grid scale, rather than a constant planting area map and fixed growing period. Such dynamic information assisted us in capturing better spatial and temporal variations in rice yields, and consequently greatly improved the accuracy of our product. Moreover, we applied four predictor categories and the optimal ML models to estimate seasonal yields. Four predictor categories provided comprehensive rice growth information to ensure the accuracy of yield estimations. The optimal

models for each rice season are determined by the IPW method. As a weighted ensemble assessment to fully consider training, validation, and testing accuracy, we are certain that the IPW method is more robust and reasonable to select the optimal model for seasonal rice yield in Asia.

4.3 Uncertainty analysis

For the spatial uncertainty, the *RRMSE* values in most areas were below 30%, indicating the low uncertainty of AisaRiceYield4km. High uncertainty of *RRMSE* (above 50%) was distributed in northeastern China and western India for single rice and central Bangladesh for winter season of triple rice (Fig. 10).

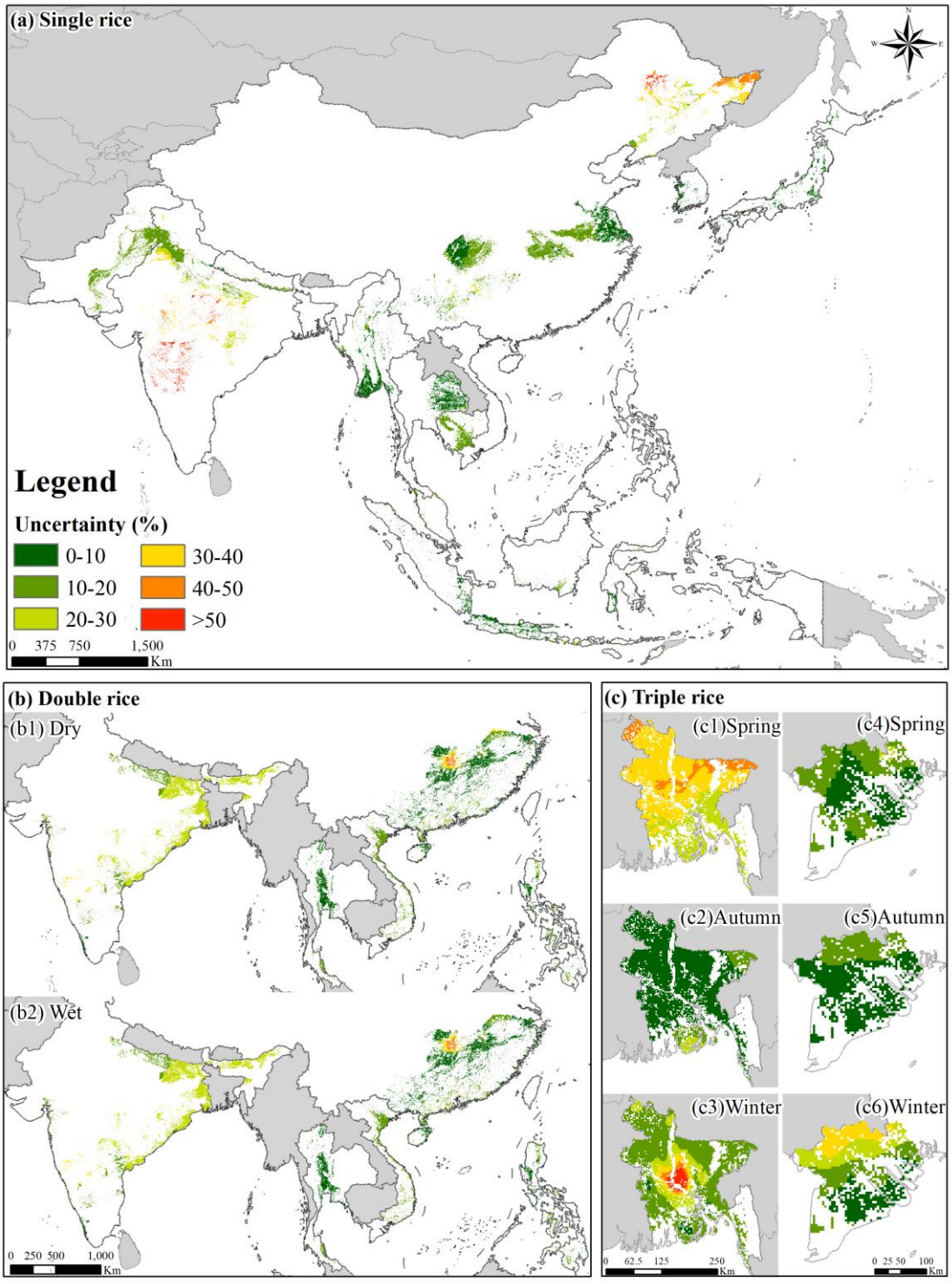

Figure 10: Spatial distribution of uncertainty (*RRMSE*, %) in AsiaRiceYield4km.

In this study, we have improved the yield prediction processes to ensure the accuracy of the AsiaRiceYield4km product as much as possible, however, several factors might negatively impact its accuracy. Due to the limitations of remote sensing techniques (e.g., clouds and topography), some paddy rice areas cannot be recognized, consequently leading to map errors (Han et al., 2022). Besides, the rice

areas before 20000 based on the union rice area of 2000 – 2002 was also introduces some uncertainty due to the unavailable of these rice areas. The spatial resolutions of multi-source data also cause uncertainties. For example, given that the rice planting areas in Asia are always fragmented (Lowder et al., 2016) but the LAI resolution in this study is somehow coarser (0.05°), the mixed-pixel problem will inevitably influence the accuracy of AsiaRiceYield4km in small size rice-planting areas. Although the GLASS LAI has highest accuracy and lowest uncertainty and we have made several efforts to mitigate the uncertainty, there is still uncertainty and inevitable effects on the rice yield estimation (Liu et al., 2018; Li et al., 2018; Fang et al., 2019; Chen et al., 2020). In addition, the crop intensity used in this study is administrative scale. The annual crop intensity variation in rice still inflects the yield estimation results. Finally, due to the lack of a process-based mechanism, ML is weakly traceable and interpretable for rice yield variability (Muruganantham et al., 2022), especially for extreme rice yields. Nevertheless, compared with other public products (Fig. 6), our methods still generated better seasonal rice yield predictions at a higher-spatiotemporal-resolution for a longer period.

5 Data availability

The seasonal rice yield product for Asia during the period 1995-2015 (AsiaRiceYield4km) is available at https://doi.org/10.5281/zenodo.6901968 (Wu et al., 2022). We encourage users to independently verify data products before using them.

6 Conclusions

We produced a long-term seasonal rice yield dataset with high spatiotemporal resolution on dynamic paddy rice areas in Asia by using multi-source data and ML models. Our AsiaRiceYield4km dataset has higher accuracy than other public datasets and shows more spatial consistency with the observed yield. We attributed such improvements to more dynamic information (e.g., rice area and phenological dates), full consideration of rice growth conditions, and the novel IPW method to select the optimal ML model. Moreover, we discovered that constant environmental conditions contributed the most (~45%) to rice yield prediction than other growing conditions. Predictors in REP had more impacts on yield predictions than those in WGP and VEP. Our dataset can address the lack of seasonal rice yield datasets and support studies related to agricultural production and development.

Author contributions.

Conceptualization, Z.Z and F.T.; Data curation, Y.L. and J.H.; Formal analysis: H.W. and J.Z.; Funding acquisition: J.Z., Z.Z. and F.T.; Investigation: J.C., J.H., H.W., J.Z., L.Z., and Y.L.; Methodology, J.Z. and H.W.; Software, H.W. and J.Z.; Supervision, Z.Z., F.T. and J.X.; Validation, J.Z. and J.H.; Visualization: H.W. and J.Z.; Writing – original draft preparation: H.W. and J.Z.; Writing – review & editing: J.Z., Z.Z., and Q.M. All authors have read and agreed to the published version of the manuscript.

Competing interests.

The contact author has declared that neither they nor their co-authors have any competing interests.

Disclaimer.

Publisher's note: Copernicus Publications remains neutral with regard to jurisdictional claims in published maps and institutional affiliations.

Acknowledgments.

We would like to thank the editors and anonymous reviewers for their valuable comments. And we would like to thank the support of the open project of the Key Laboratory of Environmental Change and Natural Disasters, Ministry of Education, Beijing Normal University.

Financial support.

This research was funded by the National Key Research and Development Project of China (2020YFA0608201), China National Postdoctoral Program for Innovative Talents (BX20200064), and National Natural Science Foundation of China (42061144003, 41977405, 42101095).

References

Abatzoglou, J. T., Dobrowski, S. Z., Parks, S. A., and Hegewisch, K. C.: TerraClimate, a high-resolution global dataset of monthly climate and climatic water balance from 1958–2015, Sci. Data, 5, 1–12, https://doi.org/10.1038/sdata.2017.191, 2018.

Alexandratos, N. and Bruinsma, J.: World agriculture towards 2030/2050: the 2012 revision, 2012.

Arumugam, P., Chemura, A., Schauberger, B., and Gornott, C.: Remote Sensing Based Yield Estimation of Rice (Oryza Sativa L.) Using Gradient Boosted Regression in India, Remote Sens., 13, 2379, https://doi.org/10.3390/rs13122379, 2021.

Bandumula, N.: Rice production in Asia: Key to global food security, Proc. Natl. Acad. Sci. India Sect. B Biol. Sci., 88, 1323–1328, https://doi.org/10.1007/s40011-017-0867-7, 2018.

Birla, D. S., Malik, K., Sainger, M., Chaudhary, D., Jaiwal, R., and Jaiwal, P. K.: Progress and challenges in improving the nutritional quality of rice (Oryza sativa L.), Crit. Rev. Food Sci. Nutr., 57, 2455–2481, https://doi.org/10.1080/10408398.2015.1084992, 2017.

Blomqvist, L., Yates, L., and Brook, B. W.: Drivers of increasing global crop production: A decomposition analysis, Environ. Res. Lett., 15, 0940b6, https://doi.org/10.1088/1748-9326/ab9e9c, 2020.

Breiman, L.: Bagging predictors, Mach. Learn., 24, 123–140, https://doi.org/10.1007/BF00058655, 1996.

Breiman, L.: Random forests, Mach. Learn., 45, 5–32, https://doi.org/10.1023/A:1010933404324, 2001.

Cai, Y., Guan, K., Lobell, D., Potgieter, A. B., Wang, S., Peng, J., Xu, T., Asseng, S., Zhang, Y., and You, L.: Integrating satellite and climate data to predict wheat yield in Australia using machine learning approaches, Agric. For. Meteorol., 274, 144–159, https://doi.org/10.1016/j.agrformet.2019.03.010, 2019.

Cao, J., Zhang, Z., Tao, F., Zhang, L., Luo, Y., Han, J., and Li, Z.: Identifying the Contributions of Multi-Source Data for Winter Wheat Yield Prediction in China, Remote Sens., 12, 750, https://doi.org/10.3390/rs12050750, 2020.

Cao, J., Zhang, Z., Tao, F., Zhang, L., Luo, Y., Zhang, J., Han, J., and Xie, J.: Integrating Multi-Source Data for Rice Yield Prediction across China using Machine Learning and Deep Learning Approaches, Agric. For. Meteorol., 297, 108275, https://doi.org/10.1016/j.agrformet.2020.108275, 2021.

Chang, K.-W., Shen, Y., and Lo, J.-C.: Predicting rice yield using canopy reflectance measured at booting stage, Agron. J., 97, 872–878, https://doi.org/10.2134/agronj2004.0162, 2005.

Chen, H., Zhu, G., Zhang, K., Bi, J., Jia, X., Ding, B., Zhang, Y., Shang, S., Zhao, N., and Qin, W.: Evaluation of evapotranspiration models using different LAI and meteorological forcing data from 1982 to 2017, Remote Sens., 12, 2473, https://doi.org/10.3390/rs12152473, 2020.

Chen, S., Liu, W., Feng, P., Ye, T., Ma, Y., and Zhang, Z.: Improving Spatial Disaggregation of Crop Yield by Incorporating Machine Learning with Multisource Data: A Case Study of Chinese Maize Yield, Remote Sens., 14, 2340, https://doi.org/10.3390/rs14102340, 2022.

Chen, T. and Guestrin, C.: Xgboost: A scalable tree boosting system, in: Proceedings of the 22nd acm sigkdd international conference on knowledge discovery and data mining, San Francisco, CA, USA, 13-17 August 2016, 785–794, https://doi.org/10.1145/2939672.2939785, 2016.

Chen, Y., Song, X., Wang, S., Huang, J., and Mansaray, L. R.: Impacts of spatial heterogeneity on crop area mapping in Canada using MODIS data, ISPRS J. Photogramm. Remote Sens., 119, 451–461, https://doi.org/10.1016/j.isprsjprs.2016.07.007, 2016.

Chen, Y., Zhang, Z., Tao, F., Palosuo, T., and Rötter, R. P.: Impacts of heat stress on leaf area index and growth duration of winter wheat in the North China Plain, Field Crops Res., 222, 230–237, https://doi.org/10.1016/j.fcr.2017.06.007, 2018.

Chlingaryan, A., Sukkarieh, S., and Whelan, B.: Machine learning approaches for crop yield prediction and nitrogen status estimation in precision agriculture: A review, Comput. Electron. Agric., 151, 61–69, https://doi.org/10.1016/j.compag.2018.05.012, 2018.

Dawe, D., Pandey, S., and Nelson, A.: Emerging trends and spatial patterns of rice production, in: Rice in the global economy: Strategic research and policy issues for food security, edited by: Sushil, P., Derek, B., David, D., Achim, D., Samarendu, M., Scott, R., and Bill, H., International Rice Research Institute (IRRI), Los Baños, Philippines, 15–36, 2010.

Dinh, T. L. A. and Aires, F.: Nested leave-two-out cross-validation for the optimal crop yield model selection, Geosci. Model Dev., 15, 3519–3535, https://doi.org/10.5194/gmd-15-3519-2022, 2022.

Fang, H., Zhang, Y., Wei, S., Li, W., Ye, Y., Sun, T., and Liu, W.: Validation of global moderate resolution leaf area index (LAI) products over croplands in northeastern China, Remote Sens. Environ., 233, 111377, https://doi.org/10.1016/j.rse.2019.111377, 2019.

Food and Agriculture Organization of the United Nations, FAO: https://www.fao.org/faostat/en/#data/QCL/visualize, last access: 6 April 2022.

Fernandez-Beltran, R., Baidar, T., Kang, J., and Pla, F.: Rice-yield prediction with multi-temporal sentinel-2 data and 3D CNN: A case study in Nepal, Remote Sens., 13, 1391, https://doi.org/10.3390/rs13071391, 2021.

Folberth, C., Skalskỳ, R., Moltchanova, E., Balkovič, J., Azevedo, L. B., Obersteiner, M., and Van Der Velde, M.: Uncertainty in soil data can outweigh climate impact signals in global crop yield simulations, Nat. Commun., 7, 1–13, https://doi.org/10.1038/ncomms11872, 2016.

Folberth, C., Khabarov, N., Balkovič, J., Skalskỳ, R., Visconti, P., Ciais, P., Janssens, I. A., Peñuelas, J., and Obersteiner, M.: The global cropland-sparing potential of high-yield farming, Nat. Sustain., 3, 281–289, https://doi.org/10.1038/s41893-020-0505-x, 2020.

Fritz, S., See, L., Bayas, J. C. L., Waldner, F., Jacques, D., Becker-Reshef, I., Whitcraft, A., Baruth, B., Bonifacio, R., and Crutchfield, J.: A comparison of global agricultural monitoring systems and current gaps, Agric. Syst., 168, 258–272, https://doi.org/10.1016/j.agsy.2018.05.010, 2019.

GLOBE Task Team and others: The Global Land One-kilometer Base Elevation (GLOBE) Digital Elevation Model, Version 1.0., 1999.

Han, J., Zhang, Z., Luo, Y., Cao, J., Zhang, L., Cheng, F., Zhuang, H., and Zhang, J.: APRA500: a 500 m annual paddy rice dataset for monsoon Asia using multisource remote sensing data [data set]. Zenodo., https://doi.org/10.5281/zenodo.5555721, 2021.

Han, J., Zhang, Z., Luo, Y., Cao, J., Zhang, L., Zhuang, H., Cheng, F., Zhang, J., and Tao, F.: Annual paddy rice planting area and cropping intensity datasets and their dynamics in the Asian monsoon region from 2000 to 2020, Agric. Syst., 200, 103437, https://doi.org/10.1016/j.agsy.2022.103437, 2022.

He, T., Xie, C., Liu, Q., Guan, S., and Liu, G.: Evaluation and comparison of random forest and A-LSTM networks for large-scale winter wheat identification, Remote Sens., 11, 1665, https://doi.org/10.3390/rs11141665, 2019.

Hochreiter, S. and Schmidhuber, J.: Long short-term memory, Neural Comput., 9, 1735–1780, https://doi.org/10.1162/neco.1997.9.8.1735, 1997.

Huang, J., Wang, X., Li, X., Tian, H., and Pan, Z.: Remotely sensed rice yield prediction using multi-temporal NDVI data derived from NOAA's-AVHRR, PloS ONE, 8, e70816, https://doi.org/10.1371/journal.pone.0070816, 2013.

Huntington, T., Cui, X., Mishra, U., and Scown, C. D.: Machine learning to predict biomass sorghum yields under future climate scenarios, Biofuels Bioprod. Biorefining, 14, 566–577, https://doi.org/10.1002/bbb.2087, 2020.

Iizumi, T. and Sakai, T.: The global dataset of historical yields for major crops 1981–2016, Sci. Data, 7, 97, https://doi.org/10.1038/s41597-020-0433-7, 2020.

Iizumi, T., Yokozawa, M., Sakurai, G., Travasso, M. I., Romanenkov, V., Oettli, P., Newby, T., Ishigooka, Y., and Furuya, J.: Historical changes in global yields: major cereal and legume crops from 1982 to 2006, Glob. Ecol. Biogeogr., 23, 346–357, https://doi.org/10.1111/geb.12120, 2014.

Iizumi, T., Hosokawa, N., and Wagai, R.: Soil carbon-food synergy: sizable contributions of small-scale farmers, CABI Agric. Biosci., 2, 1–15, https://doi.org/10.1186/s43170-021-00063-6, 2021.

Jeong, S., Ko, J., and Yeom, J.-M.: Predicting rice yield at pixel scale through synthetic use of crop and deep learning models with satellite data in South and North Korea, Sci. Total Environ., 802, 149726, https://doi.org/10.1016/j.scitotenv.2021.149726, 2022.

Kaltenegger, K. and Winiwarter, W.: Global gridded nitrogen indicators: influence of crop maps, Glob. Biogeochem. Cycles, 34, e2020GB006634, https://doi.org/10.1029/2020GB006634, 2020.

Kim, K.-H., Doi, Y., Ramankutty, N., and Iizumi, T.: A review of global gridded cropping system data products, Environ. Res. Lett., 16, 093005, https://doi.org/10.1088/1748-9326/ac20f4, 2021.

van Klompenburg, T., Kassahun, A., and Catal, C.: Crop yield prediction using machine learning: A systematic literature review, Comput. Electron. Agric., 177, 105709, https://doi.org/10.1016/j.compag.2020.105709, 2020.

Laborte, A. G., Gutierrez, M. A., Balanza, J. G., Saito, K., Zwart, S. J., Boschetti, M., Murty, M. V. R., Villano, L., Aunario, J. K., Reinke, R., Koo, J., Hijmans, R. J., and Nelson, A.: RiceAtlas, a spatial database of global rice calendars and production, Sci. Data, 4, 170074, https://doi.org/10.1038/sdata.2017.74, 2017.

Lambin, E. F. and Meyfroidt, P.: Global land use change, economic globalization, and the looming land scarcity, Proc. Natl. Acad. Sci., 108, 3465–3472, https://doi.org/10.1073/pnas.1100480108, 2011.

LeCun, Y., Bengio, Y., and Hinton, G.: Deep learning, Nature, 521, 436–444, https://doi.org/10.1038/nature14539, 2015.

Li, X., Lu, H., Yu, L., and Yang, K.: Comparison of the spatial characteristics of four remotely sensed leaf area index products over China: Direct validation and relative uncertainties, Remote Sens., 10, 148, 2018.

Liang, S., Cheng, J., Jia, K., Jiang, B., Liu, Q., Xiao, Z., Yao, Y., Yuan, W., Zhang, X., and Zhao, X.: The global land surface satellite (GLASS) product suite, Bull. Am. Meteorol. Soc., 102, E323–E337, https://doi.org/10.1175/BAMS-D-18-0341.1, 2021.

Lin, T.-S., Song, Y., Lawrence, P., Kheshgi, H. S., and Jain, A. K.: Worldwide Maize and Soybean Yield Response to Environmental and Management Factors Over the 20th and 21st Centuries, J. Geophys. Res. Biogeosciences, 126, e2021JG006304, https://doi.org/10.1029/2021JG006304, 2021.

Liu, C., Huang, H., and Sun, F.: A Pixel-Based Vegetation Greenness Trend Analysis over the Russian Tundra with All Available Landsat Data from 1984 to 2018, Remote Sens., 13, 4933, https://doi.org/10.3390/rs13234933, 2021a.

Liu, W., Dugar, S., McCallum, I., Thapa, G., See, L., Khadka, P., Budhathoki, N., Brown, S., Mechler, R., Fritz, S., and Shakya, P.: Integrated Participatory and Collaborative Risk Mapping for Enhancing Disaster Resilience, Isprs Int. J. Geo-Inf., 7, https://doi.org/10.3390/ijgi7020068, 2018.

Liu, W., Ye, T., Jägermeyr, J., Müller, C., Chen, S., Liu, X., and Shi, P.: Future climate change significantly alters interannual wheat yield variability over half of harvested areas, Environ. Res. Lett., https://doi.org/10.1088/1748-9326/ac1fbb, 2021b.

Lowder, S. K., Skoet, J., and Raney, T.: The number, size, and distribution of farms, smallholder farms, and family farms worldwide, World Dev., 87, 16–29, https://doi.org/10.1016/j.worlddev.2015.10.041, 2016.

Luo, Y., Zhang, Z., Chen, Y., Li, Z., and Tao, F.: ChinaCropPhen1km: a high-resolution crop phenological dataset for three staple crops in China during 2000–2015 based on leaf area index (LAI) products, Earth Syst. Sci. Data, 12, 197–214, https://doi.org/10.5194/essd-12-197-2020, 2020a.

Luo, Y., Zhang, Z., Li, Z., Chen, Y., Zhang, L., Cao, J., and Tao, F.: Identifying the spatiotemporal changes of annual harvesting areas for three staple crops in China by integrating multi-data sources, Environ. Res. Lett., 15, 074003, 2020b.

Luo, Y., Zhang, Z., Cao, J., Zhang, L., Zhang, J., Han, J., Zhuang, H., Cheng, F., and Tao, F.: Accurately mapping global wheat production system using deep learning algorithms, Int. J. Appl. Earth Obs. Geoinformation, 110, 102823, https://doi.org/10.1016/j.jag.2022.102823, 2022.

Maclean, J. L., Dawe, D. C., Hettel, G. P., and Hettel, G. P. (Eds.): Rice almanac: Source book for the most important economic activity on earth, 3rd ed., CABI Publishing, Wallingford, UK, 2002.

Manfron, G., Delmotte, S., Busetto, L., Hossard, L., Ranghetti, L., Brivio, P. A., and Boschetti, M.: Estimating inter-annual variability in winter wheat sowing dates from satellite time series in Camargue, France, Int. J. Appl. Earth Obs. Geoinformation, 57, 190–201, https://doi.org/10.1016/j.jag.2017.01.001, 2017.

Meroni, M., Waldner, F., Seguini, L., Kerdiles, H., and Rembold, F.: Yield forecasting with machine learning and small data: what gains for grains?, Agric. For. Meteorol., 308, 108555, https://doi.org/10.1016/j.agrformet.2021.108555, 2021.

Monfreda, C., Ramankutty, N., and Foley, J. A.: Farming the planet: 2. Geographic distribution of crop areas, yields, physiological types, and net primary production in the year 2000, Glob. Biogeochem. Cycles, 22, https://doi.org/10.1029/2007GB002947, 2008.

Mosleh, M. K., Hassan, Q. K., and Chowdhury, E. H.: Application of remote sensors in mapping rice area and forecasting its production: A review, Sensors, 15, 769–791, https://doi.org/10.3390/s150100769, 2015.

Muehe, E. M., Wang, T., Kerl, C. F., Planer-Friedrich, B., and Fendorf, S.: Rice production threatened by coupled stresses of climate and soil arsenic, Nat. Commun., 10, 1–10, https://doi.org/10.1038/s41467-019-12946-4, 2019.

Müller, C., Elliott, J., Kelly, D., Arneth, A., Balkovic, J., Ciais, P., Deryng, D., Folberth, C., Hoek, S., Izaurralde, R. C., Jones, C. D., Khabarov, N., Lawrence, P., Liu, W., Olin, S., Pugh, T. A. M., Reddy, A., Rosenzweig, C., Ruane, A. C., Sakurai, G., Schmid, E., Skalsky, R., Wang, X., de Wit, A., and Yang, H.: The Global Gridded Crop Model Intercomparison phase 1 simulation dataset, Sci. Data, 6, 50, https://doi.org/10.1038/s41597-019-0023-8, 2019.

Muruganantham, P., Wibowo, S., Grandhi, S., Samrat, N. H., and Islam, N.: A Systematic Literature Review on Crop Yield Prediction with Deep Learning and Remote Sensing, Remote Sens., 14, 1990, https://doi.org/10.3390/rs14091990, 2022.

Nazir, A., Ullah, S., Saqib, Z. A., Abbas, A., Ali, A., Iqbal, M. S., Hussain, K., Shakir, M., Shah, M., and Butt, M. U.: Estimation and Forecasting of Rice Yield Using Phenology-Based Algorithm and Linear Regression Model on Sentinel-II Satellite Data, Agriculture, 11, 1026, https://doi.org/10.3390/agriculture11101026, 2021.

Obsie, E. Y., Qu, H., and Drummond, F.: Wild blueberry yield prediction using a combination of computer simulation and machine learning algorithms, Comput. Electron. Agric., 178, 105778, https://doi.org/10.1016/j.compag.2020.105778, 2020.

van Oort, P. A. and Zwart, S. J.: Impacts of climate change on rice production in Africa and causes of simulated yield changes, Glob. Change Biol., 24, 1029–1045, https://doi.org/10.1111/gcb.13967, 2018.

Qian, H., Huang, S., Chen, J., Wang, L., Hungate, B. A., van Kessel, C., Zhang, J., Deng, A., Jiang, Y., and van Groenigen, K. J.: Lower-than-expected CH4 emissions from rice paddies with rising CO2 concentrations, Glob. Change Biol., 26, 2368–2376, https://doi.org/10.1111/gcb.14984, 2020.

Ray, D. K., West, P. C., Clark, M., Gerber, J. S., Prishchepov, A. V., and Chatterjee, S.: Climate change has likely already affected global food production, PloS One, 14, e0217148, https://doi.org/10.1371/journal.pone.0217148, 2019.

Ripley, B. D.: Pattern recognition and neural networks, Cambridge university press, 2007.

Sak, H., Senior, A., and Beaufays, F.: Long short-term memory based recurrent neural network architectures for large vocabulary speech recognition, arXiv [preprint], arXiv:1402.1128, 5 February 2014.

Sakamoto, T.: Incorporating environmental variables into a MODIS-based crop yield estimation method for United States corn and soybeans through the use of a random forest regression algorithm, ISPRS J. Photogramm. Remote Sens., 160, 208–228, https://doi.org/10.1016/j.isprsjprs.2019.12.012, 2020.

Sakamoto, T., Yokozawa, M., Toritani, H., Shibayama, M., Ishitsuka, N., and Ohno, H.: A crop phenology detection method using time-series MODIS data, Remote Sens. Environ., 96, 366–374, https://doi.org/10.1016/j.rse.2005.03.008, 2005.

Salvacion, A. R.: Chapter 11 - Multiscale drought hazard assessment in the Philippines, in: Computers in Earth and Environmental Sciences, edited by: Pourghasemi, H. R., Elsevier, Amsterdam, Netherlands, 169–179, 2022.

Shahhosseini, M., Hu, G., and Archontoulis, S. V.: Forecasting Corn Yield With Machine Learning Ensembles, Front. Plant Sci., 11, 1120, https://doi.org/10.3389/fpls.2020.01120, 2020.

Shahhosseini, M., Hu, G., Huber, I., and Archontoulis, S. V.: Coupling machine learning and crop modeling improves crop yield prediction in the US Corn Belt, Sci. Rep., 11, 1606, https://doi.org/10.1038/s41598-020-80820-1, 2021.

Son, N. T., Chen, C. F., Chen, C. R., Chang, L. Y., Duc, H. N., and Nguyen, L. D.: Prediction of rice crop yield using MODIS EVI- LAI data in the Mekong Delta, Vietnam, Int. J. Remote Sens., 34, 7275–7292, https://doi.org/10.1080/01431161.2013.818258, 2013.

Son, N.-T., Chen, C.-F., Chen, C.-R., Guo, H.-Y., Cheng, Y.-S., Chen, S.-L., Lin, H.-S., and Chen, S.-H.: Machine learning approaches for rice crop yield predictions using time-series satellite data in Taiwan, Int. J. Remote Sens., 41, 7868–7888, https://doi.org/10.1080/01431161.2020.1766148, 2020.

Srivastava, V. C. and Mahapatra, I. C.: Advances in Rice Production Technology: Theory and Practice, Agrobios, India, 2012.

Tian, H., Wang, P., Tansey, K., Zhang, J., Zhang, S., and Li, H.: An LSTM neural network for improving wheat yield estimates by integrating remote sensing data and meteorological data in the Guanzhong Plain, PR China, Agric. For. Meteorol., 310, 108629, https://doi.org/10.1016/j.agrformet.2021.108629, 2021.

Wang, C., Zhang, Z., Chen, Y., Tao, F., Zhang, J., and Zhang, W.: Comparing different smoothing methods to detect double-cropping rice phenology based on LAI products–a case study in the Hunan province of China, Int. J. Remote Sens., 39, 6405–6428, https://doi.org/10.1080/01431161.2018.1460504, 2018.

Wieder, W. R., Boehnert, J., Bonan, G. B., and Langseth, M.: Regridded harmonized world soil database v1. 2 ORNL DAAC [data set], https://doi.org/10.3334/ORNLDAAC/1247, 2014.

Wu, H., Zhang, J., Zhang, Z., Han, J., Cao, J., Zhang, L., Luo, Y., Mei, Q., Xu, J., and Tao, F.: AsiaRiceYield4km: Seasonal Rice Yield in Asia from 1995 to 2015 [data set]. Zenodo., https://doi.org/10.5281/zenodo.6901968, 2022.

Xiao, Z., Liang, S., Wang, J., Chen, P., Yin, X., Zhang, L., and Song, J.: Use of general regression neural networks for generating the GLASS leaf area index product from time-series MODIS surface reflectance, IEEE Trans. Geosci. Remote Sens., 52, 209–223, https://doi.org/10.1109/TGRS.2013.2237780, 2013.

Xiao, Z., Liang, S., Wang, J., Xiang, Y., Zhao, X., and Song, J.: Long-time-series global land surface satellite leaf area index product derived from MODIS and AVHRR surface reflectance, IEEE Trans. Geosci. Remote Sens., 54, 5301–5318, https://doi.org/10.1109/TGRS.2016.2560522, 2016.

Xiao, Z., Liang, S., and Jiang, B.: Evaluation of four long time-series global leaf area index products, Agric. For. Meteorol., 246, 218–230, 2017.

You, L. and Wood, S.: An entropy approach to spatial disaggregation of agricultural production, Agric. Syst., 90, 329–347, https://doi.org/10.1016/j.agsy.2006.01.008, 2006.

Yu, Q., You, L., Wood-Sichra, U., Ru, Y., Joglekar, A. K., Fritz, S., Xiong, W., Lu, M., Wu, W., and Yang, P.: A cultivated planet in 2010–Part 2: the global gridded agricultural-production maps, Earth Syst. Sci. Data, 12, 3545–3572, https://doi.org/10.5194/essd-12-3545-2020, 2020.

Zhang, G., Xiao, X., Dong, J., Xin, F., Zhang, Y., Qin, Y., Doughty, R. B., and Moore, B.: Fingerprint of rice paddies in spatial–temporal dynamics of atmospheric methane concentration in monsoon Asia, Nat. Commun., 11, 1–11, 2020a.

Zhang, J., Wu, H., Zhang, Z., Zhang, L., Luo, Y., Han, J., and Tao, F.: Asian Rice Calendar Dynamics Detected by Remote Sensing and Their Climate Drivers, Remote Sens., 13, https://doi.org/10.3390/rs14174189, 2022.

Zhang, L., Zhang, Z., Luo, Y., Cao, J., and Tao, F.: Combining Optical, Fluorescence, Thermal Satellite, and Environmental Data to Predict County-Level Maize Yield in China Using Machine Learning Approaches, Remote Sens., 12, 21, https://doi.org/10.3390/rs12010021, 2019.

Zhang, L., Zhang, Z., Luo, Y., Cao, J., Xie, R., and Li, S.: Integrating satellite-derived climatic and vegetation indices to predict smallholder maize yield using deep learning, Agric. For. Meteorol., 311, 108666, https://doi.org/10.1016/j.agrformet.2021.108666, 2021.

Zhang, T., Yang, X., Wang, H., Li, Y., and Ye, Q.: Climatic and technological ceilings for C hinese rice stagnation based on yield gaps and yield trend pattern analysis, Glob. Change Biol., 20, 1289–1298, https://doi.org/10.1111/gcb.12428, 2014.

Zhang, Z., Li, Z., Chen, Y., Zhang, L., and Tao, F.: Improving regional wheat yields estimations by multi-step-assimilating of a crop model with multi-source data, Agric. For. Meteorol., 290, 107993, https://doi.org/10.1016/j.agrformet.2020.107993, 2020b.